Coherent control of an optically injected ballistic spin-polarized current in bulk GaAs

Martin J. Stevens and Arthur L. Smirl[a)]
Laboratory for Photonics and Quantum Electronics, 138 IATL, University of Iowa, Iowa City, Iowa 52242

R. D. R. Bhat, J. E. Sipe, and H. M. van Driel
Department of Physics, University of Toronto, 60 St. George Street, Toronto, Ontario M5S 1A7, Canada

(Received 8 November 2001; accepted for publication 9 January 2002)

We demonstrate coherent all-optical injection and control of a ballistic spin-polarized current in bulk, low-temperature-grown GaAs at room temperature. The spin current is injected by interfering the two-photon absorption of the fundamental (1.55 μm) and the single photon absorption of the second harmonic (0.775 μm) of $\sim$180 fs pulses that propagate collinearly and have the same circular polarization. Adjusting the relative phase of the two pulses controls the direction of this current. The component of the electrical current transverse to the pulse propagation direction is investigated by monitoring charge collection across a pair of gold electrodes deposited on the GaAs surface. Results are in agreement with recent theoretical predictions. © *2002 American Institute of Physics.* [DOI: 10.1063/1.1456943]

I. INTRODUCTION

Present solid-state electronic devices rely on manipulating the flow of charge through semiconductor materials; however, there is a growing interest in using the spin of the charge carriers as another degree of freedom in order to increase storage capacity and computing power (so-called "spintronics").[1] One of the major hurdles in the development of spintronic devices has been the problem of injecting spin-polarized currents into a semiconductor. Much recent work has focused on electrical injection from magnetic semiconductors[2–4] or ferromagnetic contacts.[5,6] There have also been successful efforts to inject ballistic spin-polarized carrier populations into semiconductors using scanning tunneling microscopes.[7,8]

Here, we focus on the all-optical injection and the coherent control of spin-polarized currents. It has been known since the early 1970's that a spin-polarized carrier *population* (as opposed to a current) can be produced by the absorption of a monochromatic, circularly polarized optical pulse with photon energy above the direct band gap in a bulk semiconductor, such as GaAs.[9,10] The production of a carrier population with a net spin by direct absorption of circularly polarized light is a consequence of the optical selection rules for the heavy-hole and light-hole valence-to-conduction band transitions. For circularly polarized light, direct transitions from the heavy-hole valence band will produce electrons with the opposite spin from those from the light-hole band. However, the heavy-hole transition in unstrained bulk GaAs is three times stronger than the light-hole band transition, leading to a 3:1 ratio of spin-up to spin-down (or vice-versa) conduction band electrons. Consequently, optical excitation with circularly polarized light produces a 50% spin-polarized carrier population, provided the photon energy is low enough to avoid exciting carriers from the split-off band to the conduction band. Furthermore, if the degeneracy of the heavy-hole and light-hole valence bands is removed (e.g., by quantum confinement or strain) and if only the heavy-hole band is excited, 100% spin-polarized populations can be created.

A spin-polarized population produced in this way by the direct absorption of circularly polarized light will be distributed symmetrically in k space in materials with zincblende symmetry. Consequently, there can be no net electrical current without an external bias, even though each individual carrier may be injected initially with a large momentum when the material is excited well above the band gap. Such symmetric populations have been the subject of much of the work on optically injected spin-polarized carriers in semiconductors.[1,10,11] Recently, however, optically injected spin-polarized carrier populations have been pulled by an external electric field to create a spin-polarized current,[12,13] and such a current has been transferred through a barrier between two different semiconductor materials.[14]

By comparison to the work on the creation of spin-polarized populations that are *symmetric* in k space, in the mid-1990's, Atanasov *et al.*[15] predicted and Haché *et al.* demonstrated[16,17] that it is possible to optically inject a carrier population that is *asymmetric* in k space. By doing so, they generated a *ballistic electrical current* in an undoped and unbiased bulk semiconductor through the quantum interference between two different pathways connecting the same initial and final states. In initial demonstrations of this quantum interference control (QUIC),[16,17] one- and two-photon absorption processes were used to connect the same initial states in the valence bands and final states in the conduction band. By controlling the relative phase between the two beams, one can arrange for constructive interference in one direction in k space and destructive interference in another direction. This asymmetric distribution of carriers in k space leads to a ballistic current.

[a)]Electronic mail: art-smirl@uiowa.edu

 © 2002 American Institute of Physics

Downloaded 12 Jan 2004 to 128.100.93.83. Redistribution subject to AIP license or copyright, see http://ojps.aip.org/japo/japcr.jsp

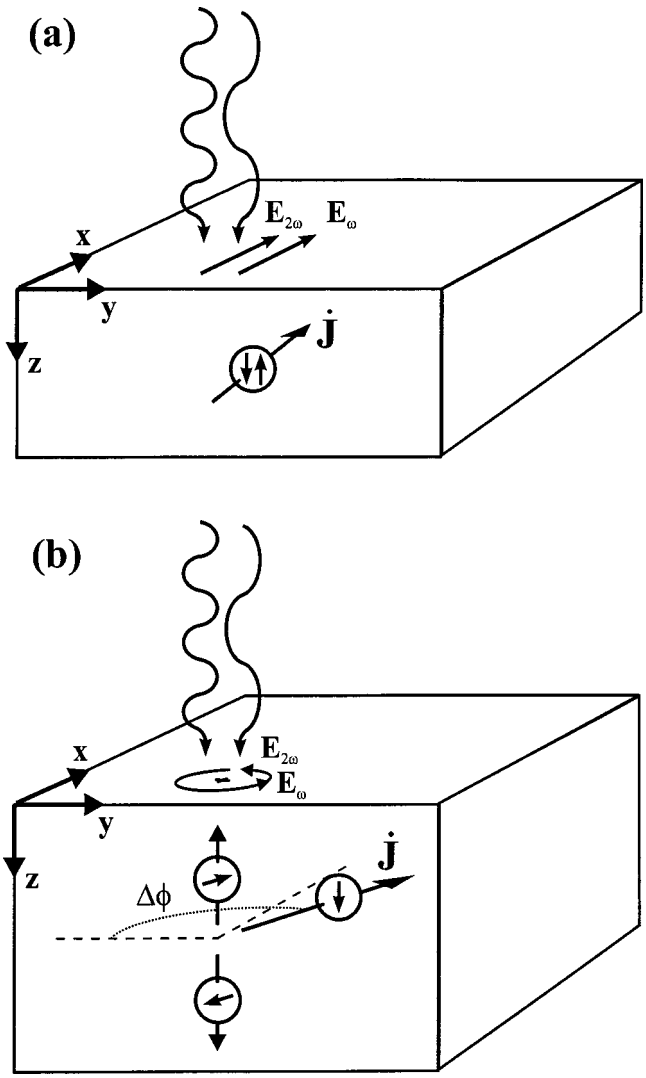

FIG. 1. (a) Schematic of electrical current injection rate ($\dot{\mathbf{J}}$) when both ω and 2ω are $\hat{x}$ polarized. The current travels in the x direction and consists of equal portions of spin-up and spin-down carriers, and thus has no net spin. (b) Spin currents generated when ω and 2ω are both $\hat{\boldsymbol{\sigma}}^{-}$ polarized. The transverse current injection rate (in the $x-y$ plane), labeled $\dot{\mathbf{J}}$, is spin polarized. The two oppositely directed longitudinal currents (along the z direction) have equal magnitudes but opposite spins, and thus, result in no net electrical current in the longitudinal direction. Small arrows inside spheres show the direction of net spin polarization, while the larger arrows intersecting the spheres show direction of ballistic current propagation. The arrows on the top surface show polarization states of the ω and 2ω fields.

In previous two-color QUIC experiments, Haché *et al.*[16,17] used second-harmonic and fundamental beams with the same linear polarization. To facilitate a direct comparison to the work to be reported here, Fig. 1(a) summarizes the expected[15] and observed[16,17] characteristics of the QUIC currents produced under these excitation conditions. Notice that a net electrical current is produced in the direction of the incident linear optical polarization. Thus, in this geometry, the optical polarization determines the direction of current flow. The magnitude and the sign of the current can be controlled coherently by adjusting the relative phase between the two incident beams. Most importantly for our discussions here, the electrical current is not spin-polarized, since one- and two-photon absorption of the two linearly polarized beams create an equal number of spin-up and spin-down carriers.

II. BALLISTIC SPIN-POLARIZED QUIC CURRENTS

More recently, Bhat and Sipe[18] have predicted that the polarization and the phase of the incident light can be used to control not only the amplitude and direction of the current, but also the orientation of the carrier spins. They showed that, with an appropriate choice of input polarizations, it should be possible to optically inject ballistic *spin-polarized* currents, either with or without accompanying electrical currents.

Bhat and Sipe[18] considered two specific geometries. The one that we consider here is shown schematically in Fig. 1(b). In this case (referred to as Case 1 in Ref. 18), the fundamental and second-harmonic beams, with frequencies ω and 2ω, respectively, have the same circular polarization. As depicted, Bhat and Sipe predict that a net electrical current will be produced in the plane perpendicular to the propagation direction of the light [i.e., in the $x-y$ plane as drawn in Fig. 1(b)]. The direction of this transverse current will be determined by the relative phase between the two incident beams, but as the phase is varied, the magnitude of the current is unchanged. Consequently, as the phase difference is varied, the current will rotate like a phasor in the $x-y$ plane. Most importantly, this current is expected to be spin polarized. (Bhat and Sipe predict a 57% spin polarization of this current in unstrained bulk GaAs.)[18] By comparison, in the direction of propagation, there will be no net electrical current; however, two oppositely directed currents with equal magnitudes but opposite spins will be produced. The direction of the spin polarization will be determined and controlled by the phase between the second-harmonic and fundamental beams. Since there is no accompanying electrical current, this longitudinal current is a pure spin current.

In this article, we confirm that the transverse current behaves as predicted in Ref. 18 and depicted in Fig. 1(b). Specifically, we show that, when exciting with ω and 2ω pulses that have the same circular polarization, an electrical current is generated whose direction depends on the relative phase of the two beams, but whose magnitude does not. For comparison, we contrast this behavior with that observed when two pulses having the same linear polarization are used. We also verify that the current is negligible when ω and 2ω have opposite circular polarizations, as predicted by Ref. 18. The longitudinal currents shown in Fig. 1(b) are not investigated here.

It should be noted that Laman *et al.*[19] have observed an optically injected current using circularly polarized light, which one would expect to be spin polarized. However, they[19] used a single color for the excitation and relied on wurtzite symmetry. The calculations by Bhat and Sipe[18] assume cubic symmetry, and hence, do not rely on a specific crystal asymmetry. There has also been a recent report[20] of a directed electric current using a spin-polarized population created by single-beam and single-color excitation of intersubband transitions in quantum wells. By contrast, the mea-

Downloaded 12 Jan 2004 to 128.100.93.83. Redistribution subject to AIP license or copyright, see http://ojps.aip.org/japo/japcr.jsp

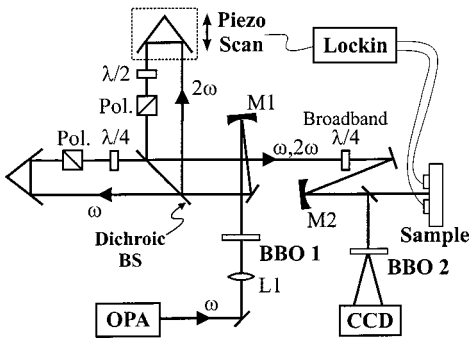

FIG. 2. Experimental geometry: BBO 1 is used for second-harmonic generation of ω (1.55 μm) into 2ω (0.775 μm); BBO 2 is used to create a cascaded $\chi^{(2)}$ signal, monitored on a CCD camera to check spatial quality of relative phase fronts of ω and 2ω; Pol. represents a polarizer; λ/2 in the 2ω arm is a zero-order half wave plate designed for 0.78 μm; λ/4 in the ω arm is a zero-order quarter wave plate designed for 1.55 μm; L1 is a lens with focal length of 10 cm; M1 and M2 are spherical curved mirrors with focal lengths of 10 cm and 5 cm, respectively.

surements we report in this article use two-color excitation of interband transitions.

III. DETECTION AND COHERENT CONTROL OF THE BALLISTIC SPIN-POLARIZED TRANSVERSE CURRENT

Because a net electrical current is produced, we can investigate the transverse current by simply collecting the charge produced by this current using conventional electrodes. The experimental geometry used to do so is shown in Figs. 2 and 3. The fundamental pulse (the ω beam), which has a pulse width of $\sim$180 fs and wavelength centered at 1.55 μm, is generated in an optical parametric amplifier (OPA) that is seeded by a Ti:Sapphire-pumped regenerative amplifier operating at 250 kHz. The second harmonic of this pulse (the 2ω beam), centered at 0.775 μm, is produced by Type-I second-harmonic generation in a BBO crystal. The two pulses are then separated using a dichroic beamsplitter, and the relative phase between the second harmonic and the fundamental is controlled by a scanning Michaelson interferometer. The polarization and intensity of each pulse are separately controlled using wave plates and polarizers in each path. The two beams are recombined collinearly, sent through a "broadband" quarter wave plate, and focused onto the space between two electrodes on the surface of a bulk, low-temperature-grown GaAs (LT-GaAs) sample. The 1.0-μm-thick layer of LT-GaAs was grown on a (001)-oriented GaAs substrate. All measurements are performed at room temperature. More details about this sample are given in Ref. 16 and references therein. For the purpose of this article, it is sufficient to note that LT-GaAs differs from normal GaAs primarily in that the excess arsenic sites in LT-GaAs lead to a shorter carrier lifetime and lower resistivity. A piezoelectric transducer attached to the retroreflector in the 2ω arm is periodically scanned to vary the phase difference between ω and 2ω, and hence to modulate the current in a given direction. We measure the voltage across the electrodes using a lock-in amplifier with this piezoelectric scanning frequency as the reference. We check that the relative phase fronts of ω and 2ω beams are constant across the beam profiles by using a cascaded $\chi^{(2)}$ process in BBO and monitoring the spatial profile of the interfering beams on a charge coupled device (CCD) camera. The experimental setup is very similar to that used by Haché *et al.*,[16] with the most significant modifications made to allow more control over the polarization states of ω and 2ω.

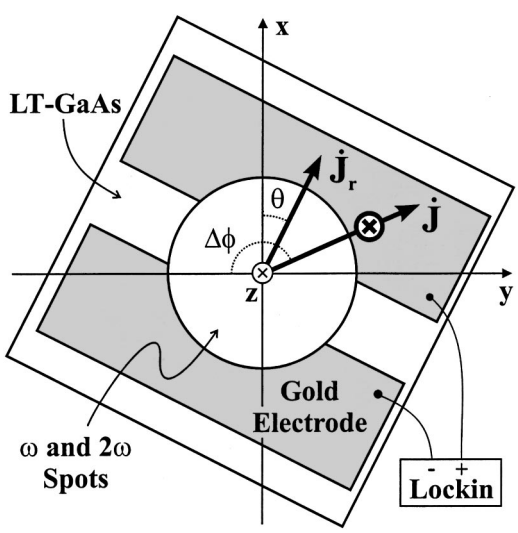

FIG. 3. Top view of the sample, a bulk, LT-GaAs sample with evaporated gold electrodes on the top surface. When ω and 2ω beams are both $\hat{\boldsymbol{\sigma}}^-$ polarized and propagate along the $+z$ direction, they generate a spin-polarized transverse electrical current in the $x-y$ plane. This current injection rate is the same $\dot{\mathbf{J}}$ as shown in Fig. 1(b). As indicated, the net spin of this current is oriented along the $+z$ direction. We can monitor the component of this transverse current along an arbitrary direction in the $x-y$ plane by choosing the sample angle θ and measuring $\dot{\mathbf{J}}_\mathbf{r}$.

Since the measurements reported here are polarization sensitive, we take care to excite with very pure polarization states. A broadband quarter wave (λ/4) plate is used to transform both ω and 2ω beams from linear to right-handed ($\hat{\boldsymbol{\sigma}}^+=(\hat{\mathbf{x}}+i\hat{\mathbf{y}})/\sqrt{2}$) or left-handed ($\hat{\boldsymbol{\sigma}}^-=(\hat{\mathbf{x}}-i\hat{\mathbf{y}})/\sqrt{2}$) circularly polarized light. However, this wave plate is not ideal. When the broadband λ/4 plate is oriented to produce left-handed circularly polarized light ($\hat{\boldsymbol{\sigma}}^-$) for linearly polarized inputs, it produces a polarization state that is 97% $\hat{\boldsymbol{\sigma}}^-$ and 3% $\hat{\boldsymbol{\sigma}}^+$ (in the field) at 0.775 μm, but only 89% $\hat{\boldsymbol{\sigma}}^-$ and 11% $\hat{\boldsymbol{\sigma}}^+$ at 1.55 μm. However, by carefully tweaking the orientations of the polarizer and quarter wave plate in the ω arm, additional retardation can be introduced, and a polarization of 99% $\hat{\boldsymbol{\sigma}}^-$ and 1% $\hat{\boldsymbol{\sigma}}^+$ can be achieved at 1.55 μm. To produce crossed circular polarizations, the broadband λ/4 plate is kept at the same angle, but the 2ω linear polarizer is rotated by 90° (resulting in a 2ω field which is 2% $\hat{\boldsymbol{\sigma}}^-$ and 98% $\hat{\boldsymbol{\sigma}}^+$). In order to excite the sample with ω and 2ω pulses having the same linear polarization ($\hat{\mathbf{x}}$), the broadband λ/4 plate is removed, and the other polarizing components are adjusted appropriately. The polarization states were measured at the sample to include the effects of all components.

We choose our photon energies such that $\hbar\omega<E_g<\hbar 2\omega$, where E_g is the band gap energy, to ensure that we create carriers through two- and one-photon absorption from ω and 2ω, respectively. We are also careful that $\hbar 2\omega<E_{\mathrm{SO}}$, where E_{SO} is the split-off band to conduction band

Downloaded 12 Jan 2004 to 128.100.93.83. Redistribution subject to AIP license or copyright, see http://ojps.aip.org/japo/japcr.jsp

energy gap, to avoid decreasing the spin polarization of our conduction band population.[9,18] The peak irradiances are $\sim 770\ \mathrm{MW/cm^2}$ (fluence $\sim 130\ \mu\mathrm{J/cm^2}$) in the ω pulse and $\sim 80\ \mathrm{MW/cm^2}$ (fluence $\sim 9\ \mu\mathrm{J/cm^2}$) in the 2ω pulse. Acting independently, the ω and 2ω pulses would create carrier densities of $\sim 2\times 10^{15}\ \mathrm{cm^{-3}}$ and $\sim 5\times 10^{17}\ \mathrm{cm^{-3}}$ through two- and one-photon absorption, respectively.

Figure 3 illustrates a view of the sample, looking along the propagation ($\hat{z}$) direction. The ω and 2ω beams are focused to full-width-half-maximum spot diameters of $\sim 50\ \mu$m and $\sim 25\ \mu$m, respectively, and the electrodes are spaced 10 μm apart. Because of the astigmatism inherent in using a curved mirror to focus onto the sample, we place the sample at a z-axis position between the vertical and horizontal waists, where the spots are roughly circular. As drawn, the sample can be rotated to allow measurement of the current along an arbitrary direction.

The qualitative behavior of the transverse current injection rate ($\dot{\mathbf{J}}$) is also depicted in Fig. 3. In Ref. 18, symmetry arguments and an eight-band Kane model are used to calculate the electrical current injection rate when both excitation pulses are $\hat{\boldsymbol{\sigma}}^-$ polarized

$$\dot{\mathbf{J}}^I_{\sigma^-\sigma^-} = \dot{J}^I_0[\sin(\Delta\phi)\hat{\mathbf{x}} - \cos(\Delta\phi)\hat{\mathbf{y}}], \tag{1}$$

where $\Delta\phi \equiv 2\phi_\omega - \phi_{2\omega}$, and ϕ_ω ($\phi_{2\omega}$) is the phase of the fundamental (second-harmonic) beam. The quantity $\dot{J}^I_0$ is given in detail in Ref. 18 (although slightly different notation is used), but for our purposes, it is sufficient to note that it is a function of the field amplitudes and GaAs material parameters, but is independent of $\Delta\phi$. It is clear from the form of Eq. (1) that the current is a constant amplitude phasor that begins along the $-y$ axis and rotates clockwise in the $x-y$ plane with increasing phase difference $\Delta\phi$.

In addition, the component of the current injection rate in any arbitrary radial direction indicated by the unit vector $\hat{\mathbf{r}} = \cos\theta\hat{\mathbf{x}} + \sin\theta\hat{\mathbf{y}}$ (where θ is measured in the clockwise direction from the x axis) is:

$$(\dot{\mathbf{J}}^I_{\sigma^-\sigma^-}\cdot\hat{\mathbf{r}})\hat{\mathbf{r}} = \dot{J}^I_0[\sin(\Delta\phi - \theta)]\hat{\mathbf{r}}. \tag{2}$$

This component of the current injection can be readily monitored by rotating the sample to the same angle θ and by measuring the voltage across the electrodes. If Eq. (2) and the description given in Ref. 18 are correct, then the peak amplitude of this current (and hence of the measured voltage) should be independent of the orientation of the electrodes; however, the maximum voltage for each orientation will occur at a unique phase difference given by $\Delta\phi = \theta + \pi/2$.

IV. RESULTS AND DISCUSSION

The measured peak amplitude of the signal as a function of the sample orientation θ is shown by the solid squares in Fig. 4 for second-harmonic and fundamental pulses having the same left-handed circular polarization. The amplitude is constant to within 10% of the mean. The dependence of this current on the phase difference $\Delta\phi$ at two fixed sample orientations is illustrated in Fig. 5(a). The solid triangles are the results of measuring the voltage as a function of the phase difference $\Delta\phi$ with the electrodes oriented to measure the current along the x direction ($\theta = 0°$), and the solid circles are the results with the sample rotated to measure the current along the y direction ($\theta = 90°$). As predicted, notice that both x and y signals vary sinusoidally with $\Delta\phi$; the peak amplitudes are equal; and the two curves are out of phase by approximately 90°.

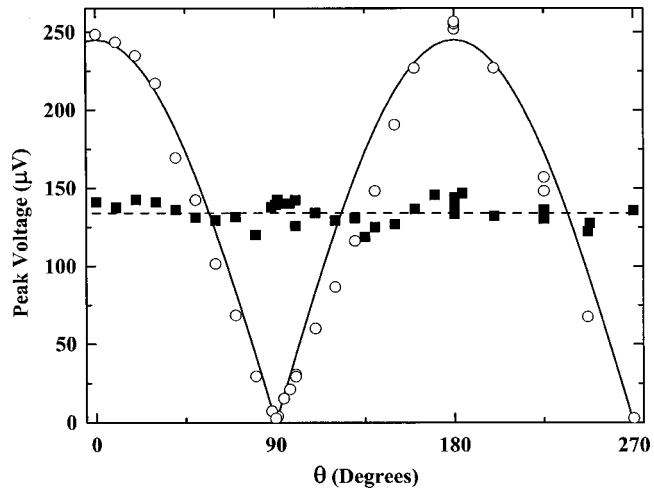

FIG. 4. Peak voltage as a function of sample angle, θ. The solid squares are taken with ω and 2ω both $\hat{\boldsymbol{\sigma}}^-$ polarized, and the open circles are taken with ω and 2ω both $\hat{\mathbf{x}}$ polarized. To remove any offset voltage, we take the peak voltage to be one half the peak-to-peak voltage, which is always positive.

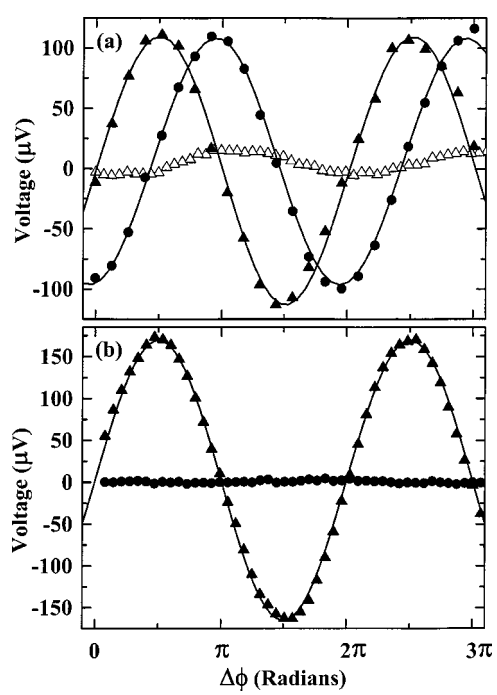

FIG. 5. Measured electrical currents along the x (triangles) and y (circles) directions as a function of the phase difference $\Delta\phi$ between the fundamental (ω) and the second harmonic (2ω) beams: (a) for the same ($\hat{\boldsymbol{\sigma}}^-$) circular polarization (solid triangles and circles) and for opposite circular polarizations (open triangles, y-direction not shown for clarity) and (b) for the same linear ($\hat{\mathbf{x}}$) polarizations for the ω and 2ω beams. Solid lines are sinusoidal fits to the data. The data shown in this figure were taken with slightly lower irradiances than the data in Fig. 4.

Downloaded 12 Jan 2004 to 128.100.93.83. Redistribution subject to AIP license or copyright, see http://ojps.aip.org/japo/japcr.jsp

The model given in Ref. 18 also predicts that there should be no transverse current for opposite circular polarizations. As confirmation of this prediction, the open triangles in Fig. 5(a) represent measurements of the x component of the signal for the ω beam $\hat{\boldsymbol{\sigma}}^-$ polarized and the 2ω beam $\hat{\boldsymbol{\sigma}}^+$ polarized. This signal almost completely disappears. We also measured the y component (not shown), and it has about the same magnitude as the x component. The small remaining signal in the case of crossed circular polarizations may be a result of our inability to create perfectly circularly polarized light.

By contrast, when both excitation pulses are linearly polarized along the $\hat{\mathbf{x}}$ direction, the coherently injected ballistic current behaves very differently and is of the form[17,18]

$$\dot{\mathbf{J}}^I_{xx} = \sqrt{2}\dot{J}^I_0 \sin(\Delta\phi)\hat{\mathbf{x}}. \tag{3}$$

That is, the current is always in the direction of the incident polarization, the magnitude is controlled by the phase, and the projection along an arbitrary direction $\hat{r}$ is proportional to the cosine of the angle of rotation:

$$(\dot{\mathbf{J}}^I_{xx}\cdot\hat{\mathbf{r}})\hat{\mathbf{r}} = \sqrt{2}\dot{J}^I_0 \sin(\Delta\phi)\cos\theta\hat{\mathbf{r}}. \tag{4}$$

For comparison with the same circular polarization data, this behavior is also illustrated in Figs. 4 and 5(b). The open circles in Fig. 4 show that the peak signal in any direction is indeed proportional to the magnitude of $\cos\theta$. (Peak signal is always positive.) The solid triangles in Fig. 5(b) show that the current in the x direction varies sinusoidally, but the solid circles indicate that there is no current along the y direction, in agreement with Eq. (3). Curves similar to those shown in Fig. 5(b) [but not Fig. 5(a)] have been published previously;[16] we show our same linear excitation data here to ensure a self-consistent comparison with our same circular excitation data.

The relative magnitudes of the two curves in Fig. 4 suggest that the maximum current in the x direction for same linear excitation is ~ 1.8 times larger than the maximum for same circular excitation. This ratio is in fairly good agreement with Eqs. (1) and (3) and the model in Ref. 18, which predict that the current for same linear excitation should be larger by a factor of $\sqrt{2}$. In addition, a slightly higher irradiance was used for the same linear polarization measurements than for the same circular polarization measurements, so the actual ratio is probably smaller than 1.8.

The amplitudes and relative phases of the x and y currents for $\hat{\boldsymbol{\sigma}}^-\hat{\boldsymbol{\sigma}}^-$ excitation can be inferred from the data in Fig. 5(a), but the absolute phases were not determined. No relative comparison should be made between the phases of curves in Fig. 5(a) and those in 5(b), as the relative phase differences between the **xx** and the $\hat{\boldsymbol{\sigma}}^-\hat{\boldsymbol{\sigma}}^-$ curves were not calibrated.

V. SUMMARY

Together, Figs. 4 and 5 show that the interference between fundamental and second-harmonic beams having the same circular polarization produces a net in-plane transverse current that has all of the salient features of the spin-polarized transverse current described in Ref. 18. Specifically, the magnitude of this current is independent of the phase difference between the fundamental and second-harmonic beams, but the direction rotates periodically in the transverse plane with this phase difference. The present experiment does not measure the spin properties of the current directly. However, it is well known that either single- or two-photon absorption of circularly polarized light alone will produce a spin-polarized carrier population, even when exciting well above the band gap,[9,10,21,22] and certainly within the context of the model given by Ref. 18, the carriers responsible for this current must be spin polarized. This experiment is an important first step in the all-optical control of spin currents in semiconductors.

ACKNOWLEDGMENTS

The authors gratefully acknowledge insightful conversations with Daniel Côté, Eric Gansen, Scot Hawkins, Yaser Kerachian, Norman Laman, and Wolfgang Rühle. This work was supported in part by the Office of Naval Research, the Defense Advanced Research Projects Agency, Photonics Research Ontario, and the National Science and Engineering Research Council of Canada.

[1] D. D. Awschalom and J. M. Kikkawa, Phys. Today **52**, 33 (1999).
[2] M. Oestreich, J. Hübner, D. Hägele, P. J. Klar, W. Heimbrodt, W. W. Rühle, D. E. Ashenford, and B. Lunn, Appl. Phys. Lett. **74**, 1251 (1999).
[3] R. Fiederling, M. Keim, G. Reuscher, W. Ossau, G. Schmidt, A. Waag, and L. W. Molenkamp, Nature (London) **402**, 787 (1999).
[4] Y. Ohno, D. K. Young, B. Beschoten, F. Matsukura, H. Ohno, and D. D. Awschalom, Nature (London) **402**, 790 (1999).
[5] P. R. Hammar, B. R. Bennett, M. J. Yang, and M. Johnson, Phys. Rev. Lett. **83**, 203 (1999).
[6] S. Gardelis, C. G. Smith, C. H. W. Barnes, E. H. Linfield, and D. A. Ritchie, Phys. Rev. B **60**, 7764 (1999).
[7] S. F. Alvarado and P. Renaud, Phys. Rev. Lett. **68**, 1387 (1992).
[8] V. P. LaBella, D. W. Bullock, Z. Ding, C. Emery, A. Venkatesan, W. F. Oliver, G. J. Salamo, P. M. Thibado, and M. Mortazavi, Science **292**, 1518 (2001).
[9] M. I. Dyakonov and V. I. Perel, in *Optical Orientation*, edited by F. Meier and B. P. Zakharchenya, Modern Problems in Condensed Matter Sciences Vol. 8 (North–Holland, Amsterdam, 1984), Chap. 2.
[10] D. T. Pierce and F. Meier, Phys. Rev. B **13**, 5484 (1976).
[11] A. P. Heberle, W. W. Rühle, and K. Ploog, Phys. Rev. Lett. **72**, 3887 (1994).
[12] D. Hägele, M. Oestreich, W. W. Rühle, N. Nestle, and K. Eberl, Appl. Phys. Lett. **73**, 1580 (1998).
[13] J. M. Kikkawa and D. D. Awschalom, Nature (London) **397**, 139 (1999).
[14] I. Malajovich, J. J. Berry, N. Samarth, and D. D. Awschalom, Nature (London) **411**, 770 (2001).
[15] R. Atanasov, A. Haché, J. L. P. Hughes, H. M. van Driel, and J. E. Sipe, Phys. Rev. Lett. **76**, 1703 (1996).
[16] A. Haché, J. E. Sipe, and H. M. van Driel, IEEE J. Quantum Electron. **34**, 1144 (1998).
[17] A. Haché, Y. Kostoulas, R. Atanasov, J. L. P. Hughes, J. E. Sipe, and H. M. van Driel, Phys. Rev. Lett. **78**, 306 (1997).
[18] R. D. R. Bhat and J. E. Sipe, Phys. Rev. Lett. **85**, 5432 (2000).
[19] N. Laman, A. I. Shkrebtii, J. E. Sipe, and H. M. van Driel, Appl. Phys. Lett. **75**, 2581 (1999).
[20] S. D. Ganichev, E. L. Ivchenko, S. N. Danilov, J. Eroms, W. Wegscheider, D. Weiss, and W. Prettl, Phys. Rev. Lett. **86**, 4358 (2001).
[21] J. B. Stark, W. H. Knox, and D. S. Chemla, Phys. Rev. Lett. **68**, 3080 (1992).
[22] A. R. Bungay, S. V. Popov, I. R. Shatwell, and N. I. Zheludev, Phys. Lett. A **234**, 379 (1997).

Downloaded 12 Jan 2004 to 128.100.93.83. Redistribution subject to AIP license or copyright, see http://ojps.aip.org/japo/japcr.jsp